ELSEVIER

Journal of Organometallic Chemistry 579 (1999) 391–403

Journal of Organo metallic Chemistry

Synthesis, redox chemistry, molecular and electronic structure of some cyclopentadienylcobalt pentafulvene complexes

Hubert Wadepohl *, Franz-Josef Paffen, Hans Pritzkow

Anorganisch-chemisches Institut der Ruprecht-Karls-Universität, Im Neuenheimer Feld 270, D-69120 Heidelberg, Germany

Received 19 November 1998

Abstract

The pentafulvene complexes $[(C_5R_5)Co(C_6H_4R'R'')]$ **3d** (R = H, R′ = Me, R″ = Ph), **3f** (R = H, R′ = Ph, R″ = $C_6H_4NO_2$-4), **3g** (R = H, R′ = R″ = SMe) and **9** (R = Me, R′ = R″ = Ph) were prepared from the respective fulvenes and $[(C_5R_5)Co(C_2H_4)_2]$ **8a**,**b**. Protonation of **3** occurs at the fulvene C-α to give substituted cobaltocenium cations. The crystal and molecular structures of **3g**, **9** and of the protonation product $[\mathbf{3e}+H]^+$ (R = R′ = Ph) were determined. In the neutral complexes the non-planar fulvene ligands are essentially η^4-coordinated with short uncoordinated exocyclic carbon–carbon double bonds. In contrast, the protonated species exhibit η^5-coordinated planar five-membered rings. Using cyclic voltammetry, the complexes **3e**,**f** and **9** were shown to reversibly undergo one-electron oxidation and reduction reactions to give the cations $[\mathbf{3e}]^+$, $[\mathbf{3f}]^+$, $[\mathbf{9}]^+$ and anions $[\mathbf{3e}]^-$, $[\mathbf{3f}]^-$, $[\mathbf{9}]^-$. Complex **3g** also forms an anion $[\mathbf{3g}]^-$, but oxidation is irreversible. The X-band ESR spectra of $[\mathbf{3e}]^-$, $[\mathbf{3e}]^+$ and of $[\mathbf{9}]^-$, $[\mathbf{9}]^+$ were recorded. In marked contrast to the cations, the anion radicals exhibit considerable anisotropy of the g and A tensors. d-Electron spin densities $\rho^d = 0.5$ for the radical anions were derived from a detailed analysis and simulation of the ESR spectra. Using extended Hückel and Fenske–Hall MO calculations for the model complex $[(C_5H_5)Co(C_5H_4CH_2)]$ **3h**, the ESR and electrochemical properties were explained by the different metal participation in the HOMO (= SOMO of the cation radicals) and LUMO (= SOMO of the anion radicals). © 1999 Elsevier Science S.A. All rights reserved.

Keywords: Cyclopentadienylcobalt pentafulvene complexes; X-ray crystal structure; Cyclic voltammetry; EPR; Fenske–Hall MO calculations

---

1. Introduction

According to spectroscopic and theoretical evidence, the ground state of pentafulvenes is adequately described by the classical cross-conjugated structure **1**(**A**) [1]. However, the chemical reactivity of these polyolefins is more readily understood when a high polarizability in the direction of **1**(**B**) is assumed [2]. The resonance structure **1**(**C**) is unfavorable, due to the anti-aromaticity of the five-membered ring system.

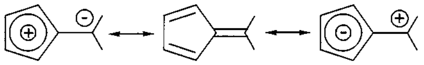

1(C) 1(A) 1(B)

Pentafulvenes have a rich organometallic chemistry, and a wide variety of types of metal complexes are known [3]. With 14 valence electron (VE) organometallic fragments, fulvene complexes with essentially η^4-coordination of the ring are formed. Structurally characterized systems include the iron [4,5], cobalt [6–9], rhodium [7] and nickel [5] complexes **2**–**5**. There appears to be no tendency of the fulvene ligands in these complexes to attain an η^5-coordination to the metal, which would imply a strong polarization of the fulvene ligand, as in **1**(**B**) or **1**(**C**).

---

* Corresponding author. Tel.: +49-6221-544827; fax: +49-6221-544197.

E-mail address: bu9@ix.urz.uni-heidelberg.de (H. Wadepohl)

PII: S0022-328X(99)00033-9

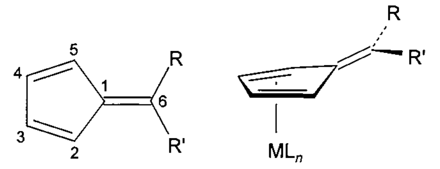

1	R	R'
a	Me	Me
b	Me	Et
c	Et	Et
d	Me	Ph
e	Ph	Ph
f	$C_6H_4NO_2$-4	Ph
g	SMe	SMe
h	H	H

	ML$_n$
2	$(CO)_3Fe$
3	$(\eta\text{-}C_5H_5)Co$
4	$(\eta^5\text{-}C_9H_7)Rh$
5	(1,5-cod)Ni
9	$(\eta\text{-}C_5Me_5)Co$

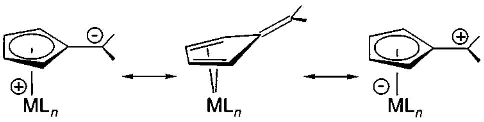

In contrast, the dinuclear ‘cobaltafulvene’ complexes **6** were found to have structures more like the zwitterion **6**(**B**) than the carbene complex **6**(**A**) [10]. These complexes are related to **3**, via the isolobal relationship of the fragments CR_2 and $Co(L)(C_5R_5)$.

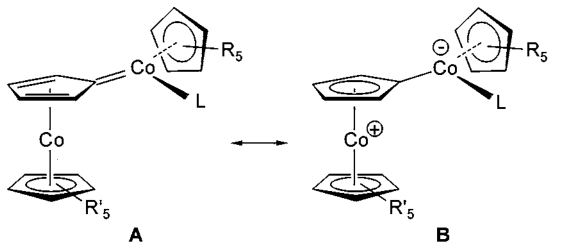

6, R, R' = H, Me; L = C_2H_4, CO, PR_3, CNR, Br

Recently, we reported on the unexpected formation of (1,1,2,2-tetramethyl-1,2-ethanediyl)bis(cobaltocene) **7** when 6,6-dimethylfulvene **1a** was treated with the Jonas reagent $[(C_5H_5)Co(C_2H_4)_2]$ **8a** [9].

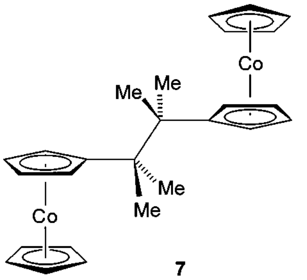

7

Apparently, the likely intermediate **3a** (R = R′ = Me) is unstable and dimerizes to give **7**. In contrast, other derivatives of **3**, including $[(C_5H_5)Co$(6-methyl-6-ethylfulvene)] **3b** and $[(C_5H_5)Co$(6,6-diethylfulvene)] **3c**, could be prepared and did not show any tendency to dimerize [9]. Here we describe further investigations of the synthesis, redox chemistry and molecular and electronic structure of fulvene complexes of the type $[(C_5R_5)Co$(pentafulvene)].

2. Results and discussion

2.1. Syntheses and spectra

The complex **3e** (R = R′ = Ph) was first prepared in situ from $[(C_5H_5)Co(CO)_2]$ and 6,6-diphenyl fulvene **1e** at 140°C [11]. This synthesis is much improved when **8a** is used as a source of the $(C_5H_5)Co$ fragment [6,7]. In the same way, the new complexes **3d** (R = Me, R′ = Ph), **3f** (R = $C_6H_4NO_2$-4, R′ = Ph) and **3g** (R = R′ = SMe) were prepared in 10–60% yield from **8a** and the respective fulvenes. Likewise, the pentamethylcyclopentadienyl complex **9** was obtained in 65% yield from $[(C_5Me_5)Co(C_2H_4)_2]$ **8b** and **1e**.

Most of the fulvene complexes are very air sensitive deep red solids or oils, except **3f**, which has a deep blue colour. The latter complex was only obtained in rather low yield. Separation from decomposition products was very tedious, due to the low solubility of **3f** and its high sensitivity. All the complexes **3** rapidly decompose when deposited on chromatography columns (SiO_2 or Al_2O_3/5% H_2O). Treatment with strong acids resulted in the formation of the substituted cobaltocenium salts $[(C_5R''_5)Co\{C_5H_4C(H)RR'\}]^+$.

Attempts to prepare $(C_5H_5)Co$ complexes with 6-phenylfulvene, 6,6-bis(nitro)fulvene and hexaphenylfulvene were not successful. In all cases, decomposition to dark intractable residues took place when the ligands were treated with **8a** at room temperature or heated with $[(C_5H_5)Co(CO)_2]$.

The NMR spectra of the complexes **3** and **9** show the usual high field coordination shifts of the fulvene ring protons, which resonate in the range $3.9 \leq \delta \leq 4.7$. Consistent with the asymmetry of the respective fulvenes, a separate resonance appears for each of the four unisochroneous fulvene ring protons of **3d** and **3f**. In the more symmetric **3g** and **9** these protons form a $(AB)_2$ spin system, which appears as two pseudo-triplets in **9**. In **3g**, both signals coincide and only one multiplet of relative intensity 4 is observed. The coordination shifts in **9** [$\Delta\delta = 2.3$ (H-2, H-5), 1.7 (H-3, H-4)] are somewhat larger than those in **3e** ($\Delta\delta = 1.9$, 1.19), consistent with the stronger electron donor properties of the $(C_5Me_5)Co$ fragments compared with $(C_5H_5)Co$. However, similar coordination shifts ($\Delta\delta = 2.6$, 1.6) were found for the fulvene ring protons in **2** (R = R′ = Ph) [5], despite the quite different donor/acceptor properties of the $(CO)_3Fe$ and $(C_5Me_5)Co$ fragments.

High field shifts on coordination are also observed for the resonances of the fulvene carbons C1 to C6. Consistent with an essentially η^4-coordination of the five-membered rings, the shifts are much stronger for C2 to C5 than for the non-coordinated C1 and C6. Unfortunately, reliable carbon spectra of **3f** could not be obtained, due to the low solubility of this complex.

*2.2. Crystal and molecular structure of $[(C_5H_5)Co(C_5H_4C(SMe)_2)]$ (**3g**), $[(C_5Me_5)Co(C_5H_4CPh_2)]$ (**9**) and $[(C_5H_5)Co(C_5H_4C(H)Ph_2)]^+$ $[PF_6]^-$ ($[$**3e**$ + H]^+$)*

Single crystal X-ray structure determinations were carried out for the fulvene complexes **3g**, **9** and for the diorganylmethyl substituted cobaltocenium cation $[$**3e**$ + H]^+$. Crystallographic details are described in the Section 3. Important bond lengths and angles are given in Tables 1 and 2.

The gross molecular structures of **3g** and **9** (Figs. 1 and 2) are quite similar and closely resemble the previously published [8] structure of **3e**. In all cases, the fulvene ligand binds to the cobalt in essentially η^4-fashion via its endocyclic 1,3-diene system. This type of coordination is invariably present in all structurally characterized pentafulvene complexes with a 14 VE metal ligand fragment (Table 3). As usual in metal complexes of 1,3-dienes, the metal carbon bonds involving the 'inner' diene carbon atoms C3 and C4 are somewhat shorter than those involving the 'outer' diene carbons C2 and C5. In the free pentafulvenes, the observed pattern of endocyclic carbon–carbon bond lengths are in accord with a polyene structure [15]. In complexes **3e**,**g** and **9**, this bond length alternation is much less pronounced within the five-membered ring. In contrast, the exocyclic bond C1–C6 is quite short both in the free ligands and in the complexes.

The fulvene ligands are folded along C2···C5, to move C1 and the exocyclic carbon–carbon bond away

Table 1
Selected bond lengths (Å) and angles (°) for the complexes $[(C_5R_5)Co(C_6H_4R'_2]$ **3g** (R = H, R′ = SMe) and **9** (R = Me, R′ = Ph)[a]

	3g	**9**
Co(1)–C(2/5)	2.057(4)/2.058(4)	2.081(3)/2.051(3)
Co(1)–C(3/4)	1.993(5)/1.992(5)	1.993(3)/1.971(3)
Co(1)···C(1)	2.316(4)	2.342(3)
Co(1)–C(9)···C(13)	2.033(5)–2.072(5)	
Co(1)–C(19)···C(23)		2.028(3)–2.087(3)
C(1)–C(2/5)	1.454(5)/1.458(6)	1.460(4)/1.455(4)
C(2/4)–C(3/5)	1.403(6)/1.418(6)	1.410(5)/1.418(5)
C(3)–C(4)	1.421(6)	1.409(5)
C(1)–C(6)	1.373(6)	1.389(4)
C(6)–S(1/2)	1.758(4)/1.760(4)	
C(6)–C(7/13)		1.458(4)/1.483(4)
S(1/2)–C(7/8)	1.789(5)/1.808(5)	
C(6)–C(1)–C(2/5)	128.6(4)/128.8(4)	129.3(3)/128.7(3)
C(3/4)–C(2/5)–C(1)	110.7(4)/109.7(4)	110.3(3)/110.5(3)
C(2/3)–C(3/4)–C(4/5)	107.4(4)/107.6(4)	107.3(3)/107.8(3)
C(1)–C(6)–S(1/2)	120.5(3)/120.6(3)	
C(1)–C(6)–C(7/13)		122.7(3)/119.8(3)
C(6)–S(1/2)–C(7/8)	103.3(2)/103.7(2)	
S(1)–C(6)–S(2)	118.9(2)	

[a] Estimated standard deviations in parentheses.

Table 2
Selected bond lengths (Å) and angles (°) for the complex cation $[(C_5H_5)Co\{C_5H_4C(H)Ph_2\}]$ $[$**3e**$+H]^{+a}$

Co(1)–C(1)	2.034(7)	Co(1)–C(2)	2.026(7)
Co(1)–C(3)	2.002(8)	Co(1)–C(4)	1.996(8)
Co(1)–C(5)	2.009(8)	Co(1)–C(19)···C(23)	2.001(8)–2.019(8)
C(1)–C(2)	1.416(9)	C(1)–C(5)	1.416(9)
C(1)–C(6)	1.520(9)	C(2)–C(3)	1.422(11)
C(3)–C(4)	1.402(12)	C(4)–C(5)	1.415(10)
C(6)–C(7)	1.523(9)	C(6)–C(13)	1.532(8)
C(2)–C(1)–C(5)	107.0(7)	C(5)–C(1)–C(6)	125.6(7)
C(2)–C(1)–C(6)	127.3(7)	C(1)–C(2)–C(3)	107.3(8)
C(2)–C(3)–C(4)	109.6(8)	C(3)–C(4)–C(5)	106.3(8)
C(1)–C(5)–C(4)	109.7(8)	C(1)–C(6)–C(7)	114.6(5)
C(1)–C(6)–C(13)	110.2(5)		

[a] Estimated standard deviations in parentheses.

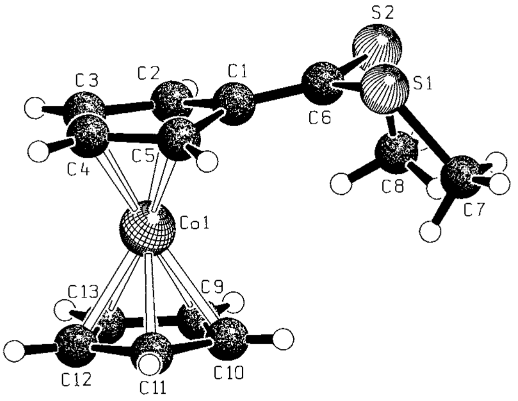

Fig. 1. Molecular structure of **3g**.

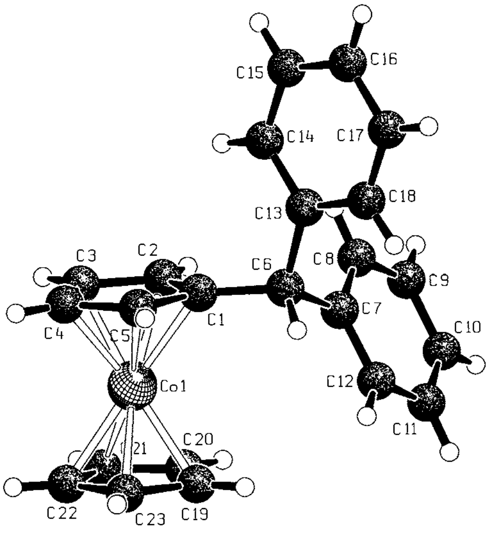

Fig. 2. Molecular structure of **9**.

Table 3
Characteristic structural parameters (distances in Å, angles in °) of some complexes of the type $[L_nM(C_5R'_4CR_2)]$

L_nM	R, R′	M–C2/5, –C3/4[a]	M···C1	C1–C6	Fold angles[b]	Ref.
$(CO)_3Fe$	Ph, H	2.142(4), 2.060(4)	2.517(4)	1.357(5)	22, −6	[5]
$(C_5H_5)Co$	Ph, H	2.043(3), 1.989(3)	2.341(3)	1.372(5)	16, −5	[8]
$(C_5H_5)Co$	SMe, H	2.058(4), 1.993(5)	2.316(4)	1.373(6)	14, −4	This work
$(C_5Me_5)Co$	Ph, H	2.066(3), 1.982(3)	2.342(3)	1.389(4)	14, −4	This work
$(Me_3P)_2(Me)Co$	C_6H_4Me-4, H	2.157(3), 2.021(3)	2.517(3)	1.382(4)	20, 0	[12]
$[(Me_3P)_3Rh]^+$	H, Me	2.248(5), 2.200(5)	2.610	1.339(7)	25, −1	[13]
(dppe)MeIr	H, Me	2.245(8), 2.188(8)	2.635(7)	1.37(1)	25, −3	[14]
(ind)Rh	$C_6H_4NMe_2$-4, H	2.193(7), 2.135(8)	2.468(7)	1.36(1)	14, −5	[7]
(cod)Ni[c]	Ph, H	2.20(1), 2.07(1)	2.43	1.37(1)	8, −2	[5]
		2.20(1), 2.07(1)	2.41	1.38(1)	10, 0	

[a] Averaged across the pseudo-mirror plane of the fulvene ligand.

[b] The first number gives the angle between the planes C2–C3–C4–C5 and C2–C1–C5; the second number gives the angle between the latter plane and the vector C1–C6.

[c] Two independent molecules.

from the metal atom. In addition, the exocyclic double bond C1=C6 is at an angle to the plane C2–C1–C5, inclined towards the metal atom (Table 3). In the cobalt fulvene complexes, the distance Co–C1 is 13–15% longer than the bonds Co–C2/C5. A similar geometry is attained by the other examples in Table 3 (10–18% difference). In the literature, there are a few complexes where cobalt carbon distances as large as 2.4 Å have been described as bonding. A clear cut case is $[\{P(OMe)_3\}_3Co(\eta^3\text{-benzyl})]$ [16] where the distance Co–C_{ortho} of 2.408(3) Å must be assumed to be bonding because of the diamagnetism of the molecule. However, for all the complexes in Table 3, a strong tendency of the fulvene ligands towards the η^4-coordination is obvious not only from the folding of the fulvene ligand, but also from the above mentioned slip of the metal atom in the η^4-coordination plane (C2–C3–C4–C5), which places the cobalt atom closer to C3 and C4.

In principle, at least part of the folding and slip of the fulvene ligands could be due to unfavourable steric interactions between the metal atom and the substituents on C6 of the fulvene. In order to get an idea of the relevance of such repulsions the molecular structures of $[\mathbf{3c}+H]^+$ and $[\mathbf{3e}+H]^+$ were determined. Unfortunately, the poor quality of the available crystals of $[\mathbf{3c}+H]^+[BPh_4]^-$ resulted in a very limited dataset. Apparent but unresolvable disorder of the ethyl groups precluded a detailed analysis of this structure. The structural parameters of the (diphenylmethyl)cyclopentadienyl ligand in $[\mathbf{3e}+H]^+$ (Fig. 3) are quite similar to those of the 1,1′-bis(benzhydryl)cobaltocenium cation [17].

In both $[\mathbf{3c}+H]^+$ and $[\mathbf{3e}+H]^+$, the C_5H_5 and the substituted cyclopentadienyl rings are planar and η^5-coordinated. There is only a minor distortion involving a barely significant lengthening of the bonds Co1–C1 and Co1–C2 (Table 2). The bulky diphenylmethyl substituent in $[\mathbf{3e}+H]^+$ causes an only slight displacement of the alpha-carbon atom C(6) from the ring plane (0.07 Å, away from the metal atom).

2.3. Redox chemistry

Cyclic voltammetry was carried out with solutions of the complexes **3e**,**f**,**g** and **9**. Relevant data are summarized in Table 4. The potential/current response for **3g** and **9** is shown in Fig. 4. The monoanions are generated by a quasi-reversible electrode process in all cases. In contrast, while reversible oxidation of **3e**,**f** and **9** is observed, oxidation of **3g** is irreversible. As the oxidation product of **3g**, a new species is formed at −0.2 V (vs. SCE), which gives rise to a new, essentially irreversible cathodic response at −0.64 V (Fig. 4).

The radical cation $[\mathbf{3g}]^+$ is obviously unstable, and decomposes probably through cleavage of a carbon sulfur bond. When generated in CH_2Cl_2 solution from

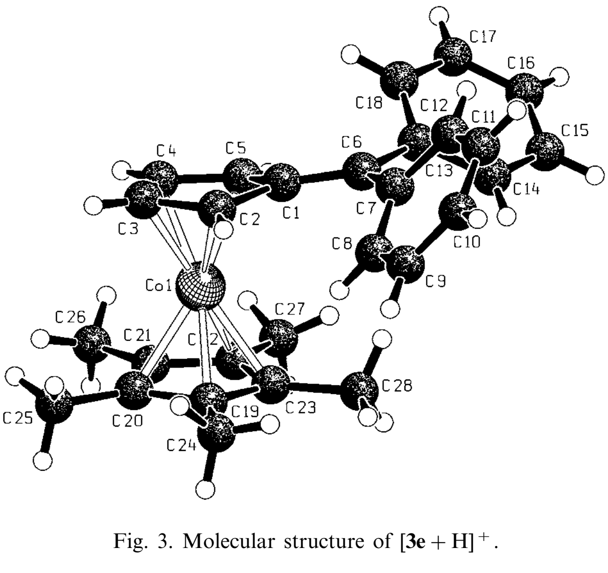

Fig. 3. Molecular structure of $[\mathbf{3e}+H]^+$.

Table 4
Cyclic voltammetry data for some complexes $[(C_5R_5)Co(C_5H_4CRR')]$[a]

	−2/−1	−1/0	0/+1	+1/+2
3e[b]	−1.88 (110)	−0.92 (80)	−0.20 (70)	+0.71 [c]
9[b]	−1.51 (140)	−1.22 (150)	−0.32 (110)	+1.57 [c]
3f[d]	−1.85 [c]	−1.16 (60)	+0.02 (50)	+0.94 [c]
3g[b]	−1.52 (110)	−0.92 (96)	−0.20 [c]	

[a] For each complex, $E°$ [V] vs. SCE is given in the first line and the peak separation ΔE_p [mV] in the second line. Supporting electrolyte: $^{n}Bu_4NPF_6$.

[b] In propylene carbonate.

[c] Irreversible.

[d] In 1,2-dimethoxyethane.

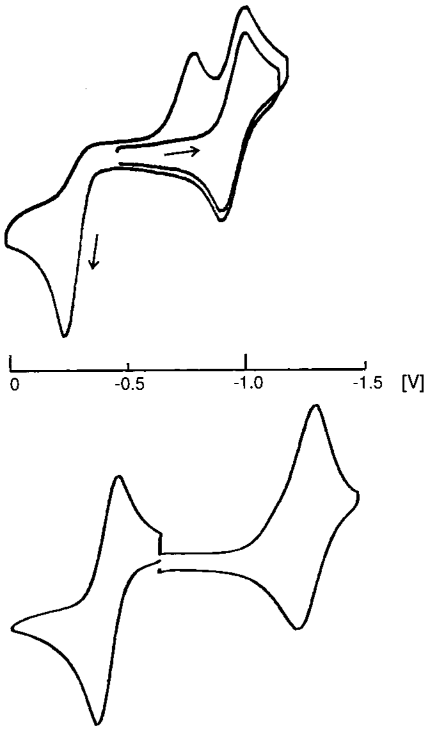

Fig. 4. Cyclic voltammogram of **3g** (top) and **9**. Solvent: propylene carbonate; supporting electrolyte: $^{n}Bu_4NPF_6$. The direction of the potential scan is indicated by arrows.

3e and $AgBF_4$ in a preparative scale, [**3e**]$^+$ also slowly decomposes. By mass spectrometry, the cobaltocenium derivatives $[(C_5H_5)Co(C_5H_4CPh_2H)]^+$ and $[(C_5H_5)Co(C_5H_4CPh_2Cl)]^+$ were detected in the decomposition products. These could be formed by hydrogen or chlorine abstraction from the solvent.

ESR resonances of [**3e**]$^-$, [**9**]$^-$ and [**3e**]$^+$, [**9**]$^+$ could be observed from samples which were partially reduced (with a potassium mirror) or oxidized (with $[(C_5H_5)_2Fe]^+[BF_4]^-$) in situ. Typical spectra, taken in frozen solutions at liquid nitrogen temperature, are depicted in Figs. 5–7. The spectra of the anions are very much alike, as are those of the cations. However, the latter are distinctly different from the former.

The resonances of the anions are indicative of a rhombic g tensor with superimposed ^{59}Co ($I = 7/2$) hyperfine structure. Part of the low field component is well resolved, and the corresponding parameters are easily obtained. The nearly equally spaced lines of this feature are an indication that at least this hyperfine tensor component shares its principal axis with the g tensor. Computer simulation resulted in the complete assignment of the spectra. The g tensor components and hyperfine splitting parameters A are given in Table 5.

For [**3e**]$^-$ an isotropic spectrum in liquid solution could also be obtained. The eight equally spaced lines of this resonance correspond to an isotropic cobalt hyperfine splitting $\langle A \rangle = 76 \times 10^{-4}$ cm^{-1}, which is close to the average of the three principle values of the hyperfine tensor, taken from Table 5. Therefore, the three components of A must have the same sign (assumed to be negative, see below). The spectra of [**3e**]$^-$ and [**9**]$^-$ are remarkably similar to those of the cyclopentadienone complexes $[(C_5H_5)Co(R_4C_4CO)]^-$

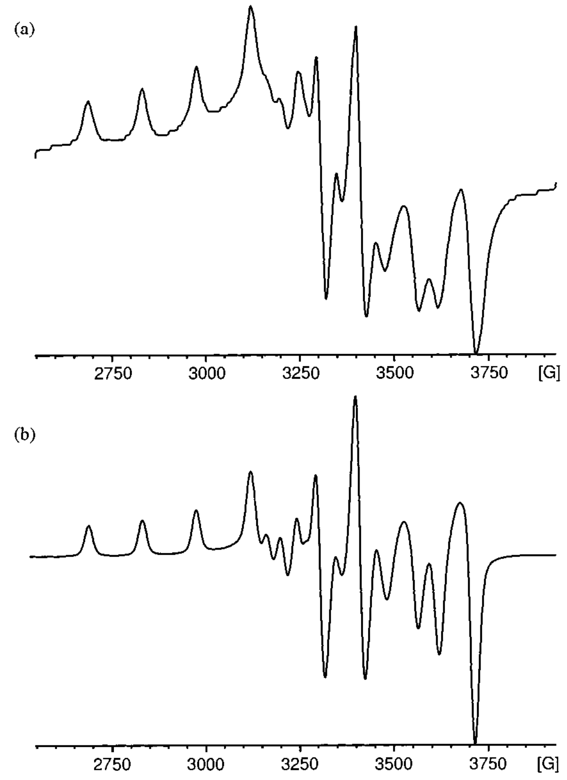

Fig. 5. (a) Experimental X-band ESR spectra of [**3e**]$^-$ in frozen THF at liquid nitrogen temperature. (b) Calculated spectrum using the parameters in Table 5.

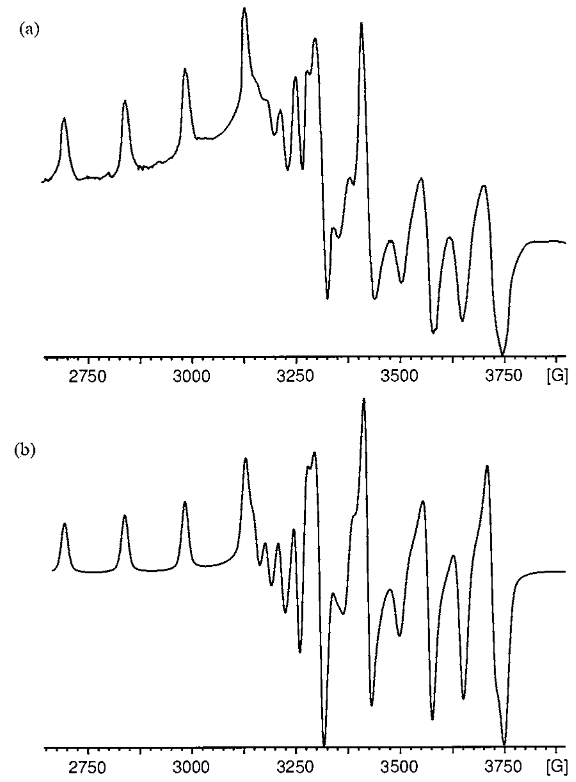

Fig. 6. (a) Experimental X-band ESR spectra of [**9**]$^-$ in frozen THF at liquid nitrogen temperature. (b) Calculated spectrum using the parameters in Table 5.

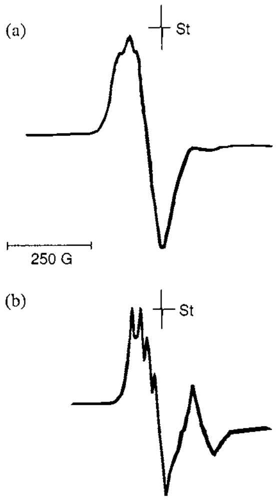

Fig. 7. Experimental X-band ESR spectra of [**3e**]$^+$ (a) and [**9**]$^+$ (b) in frozen CH_2Cl_2 at liquid nitrogen temperature. St denotes the resonance of LiTCNQ ($g = 2.0025$).

[**10**]$^-$ (R = Ph, C_6F_5) [18a]. For both types of complex, the large value of A_1 is consistent only with a large Co 3d contribution to the singly occupied molecular orbital (SOMO). Similar statements were made in a number of related cases [18b–e].

A more detailed interpretation of the ESR parameters is based on the results of the MO calculations described below. In the LCAO-MO framework, the deviation $\Delta g_i = g_i - g_e$ from the free-electron value of the g tensor components may be expressed in terms of the spin-orbit coupling parameters ζ, the spin density $\rho = a^2$, the LCAO coefficients c_{jk} and the energy difference $E_0 - E_k$ of the orbitals k relative to the SOMO with the energy E_0. The relevant expressions and their derivation are given in the literature [19]. For a primarily metal d_{yz} based SOMO, the principal g tensor components are given by

$$\Delta g_{xx} = 2\zeta_{Co}a^2 \sum_k \frac{c^2_{x^2-y^2,k} + 3c^2_{z^2,k}}{E_0 - E_k} \tag{1}$$

$$\Delta g_{yy} = 2\zeta_{Co}a^2 \sum_k \frac{c^2_{xy,k}}{E_0 - E_k} \tag{2}$$

$$\Delta g_{zz} = 2\zeta_{Co}a^2 \sum_k \frac{c^2_{xz,k}}{E_0 - E_k} \tag{3}$$

The hyperfine tensor is best expressed in terms of the isotropic coupling $\langle A \rangle$, the Fermi contact contribution A_s and the departure from axial symmetry

$$\langle A \rangle = A_s + \frac{1}{3}P(\Delta g_x + \Delta g_y + \Delta g_z) \tag{4}$$

where $P = 282 \times 10^{-4}$ cm^{-1} is the dipolar coupling constant for cobalt [20]. Combination of the expressions for g_i and A_i gives an equation to compute the 3d spin density [21] $\rho^d = a^2$

$$A_x - \langle A \rangle = P\left[-\frac{4}{7}a^2 + \frac{2}{3}\Delta g_x - \frac{5}{42}(\Delta g_y + \Delta g_z)\right] \tag{5}$$

The assignment of the experimental g_1, g_2 and g_3 to g_x, g_y and g_z is based on the following reasoning. A_x is very likely to have the same sign as $\langle A \rangle$; thus $A_x > A_y$ or A_z. This leads to $g_1 = g_x$. The orbital closest to the SOMO 13a″ is the empty 21a′ (d_{xz}) (see Fig. 8). The next closest MO, the filled 20a′ (d_{xz}) is much lower. All other filled orbitals with cobalt d contribution are at even lower energy. With this condition, Eq. (3) suggests $\Delta g_z < 0$, and therefore we can completely assign the spectra (Table 5). d-Electron spin densities ρ^d, calculated from the dipolar coupling tensor according to Eq. (5), are given in Table 6.

In our complexes, the Fermi contact coupling entirely arises from spin-polarization (A_s is therefore expected to be negative). This is because admixture of Co 4s into the SOMO belonging to the a″ representation is symmetry forbidden. In this case, ρ^d can be computed independently from the isotropic coupling by

$$A_s = Q_d \cdot \rho^d \tag{6}$$

The spin polarization coupling constant $Q_d = -131 \times 10^{-4}$ cm^{-1} for Co 3d electrons was taken from the

Table 5
ESR spectroscopic parameters (in frozen THF at 80 K) for the radical anions $[(C_5R_5)Co(6,6\text{-}Ph_2C_6H_4)]^-$ **[3e]**$^-$ (R = H), **[9]**$^-$ ($R = CH_3$) and $[(C_5H_5)Co(R_4C_5O)]^-$ ($R = Ph, C_6F_5$) **[10]**$^{-a}$

	g_x	g_y	g_z	$\langle g\rangle$	A_x	A_y	A_z	$\langle A\rangle$
[3e]$^-$	2.103	2.037	1.933	2.03[b]	(−)142	(−)43	(−)54	76[b]
[9]$^-$	2.092	2.032	1.920		(−)143	(−)38	(−)60	(−)80[c]
[10]$^{-d}$	2.103	2.025	1.906		(−)141	(−)39	(−)51	(−)77[c]

[a] Hyperfine coupling constants A are given in units of 10^{-4} cm^{-1}.

[b] From the isotropic spectrum in liquid solution at 270 K.

[c] $1/3(A_x+A_y+A_z)$.

[d] Reassigned data from ref. [18a].

literature [22]. Computed values for A_s/Q_d are also given in Table 6. The isotropic hyperfine coupling constant $\langle A\rangle = 1/3(A_x + A_y + A_z)$ can also be calculated from Eqs. (6) and (4); the values so obtained are given in the last column of Table 6. They are in reasonable agreement with the experimental values (Table 5).

Based on the above reasoning we reassigned the published [18a]. ESR spectra of the anion radicals of the cyclopentadienone complexes **[10]**$^-$. An extended Hückel MO calculation for the neutral model complex $[(C_5H_5)Co(C_5H_4O)]$ gave an ordering of molecular orbitals with metal character comparable to that in the fulvene complex **3h** [23]. In particular, the LUMO (which would be the SOMO in the anion radical) has a high contribution of d_{yz}. Assignment of the resonances as given in ref. [18a] results in $\rho^d < 0$. With our new ordering $g_x < g_y < g_z$ (Table 5), a more reasonable value of 0.53 is obtained for ρ^d, very close to that of the fulvene complexes.

'Hypervalent' formally 19 VE organometallic complexes [24] have been discussed within a continuum of the electronic structure spanning the extremes of purely metal-centered and largely ligand centered '18 + δ' radicals [25]. For example, a high metal character of the SOMO was found for the complex $[(C_5H_5)Co(1,2,5,6\text{-}\eta\text{-cycloocta-1,5-diene})]^-$ ($\rho^d = 0.68$) [18b,19]. In contrast, $[(C_5H_5)Co(1\text{-}4\text{-}\eta\text{-cycloocta-1,3,5,7-tetraene})]^-$ ($\rho^d = 0.40$) is much more delocalized [26]. In this complex, the majority of the ligand charge resides on the four carbon atoms of the uncomplexed 'butadiene-like' π-system of the cyclooctatetraene ligand. Another example of a largely ligand based 18 + δ radical appears to be the neutral $[(C_5H_5)Co(C_7H_9)]$ (C_7H_9 = cycloheptadienyl), as shown by its dimerization via formation of a carbon carbon bond between the two C_7 polyolefins [27]. In relation to the cyclooctadiene and cyclooctatetraene complexes, the fulvene (and cyclopentadienone) complexes attain an intermediate position. Generally, formation of an 18 + δ electronic structure is favoured by the presence in one of the ligands of an uncomplexed π-system, which can delocalize the unpaired electron. As indicated by the ρ^d values of about 0.5, the cross-conjugated π-system in the fulvene complex anions seems to be less efficient in that respect.

Interestingly, no stable 19 VE radicals could be obtained from a source of the 15 VE fragment $(Me_3P)_3Co$ and diarylfulvenes. Instead, upon metal coordination reductive carbon–carbon coupling takes place at the 1-positions of the fulvene C_5 rings, to give diamagnetic dinuclear (η^3-allyl)cobalt(I) derivatives (18 VE at Co) [12].

The ESR spectra of the cations show a much smaller g anisotropy (Fig. 7). Although the poorly resolved

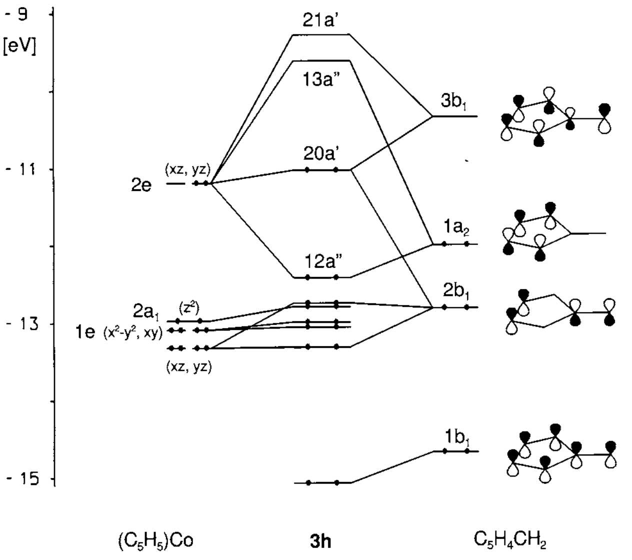

Fig. 8. Orbital interaction diagram for $[(\eta\text{-}C_5H_5)Co(\eta^5\text{-pentafulvene})]$ **3h**. The fulvene ligand is assumed to be planar.

Table 6
d-Electron spin densities for the radical anions $[(C_5R_5)Co(6,6\text{-}Ph_2C_6H_4)]^-$ **[3e]**$^-$ (R = H), **[9]**$^-$ ($R = CH_3$) and $[(C_5H_5)Co(R_4C_5O)]^-$ ($R = Ph, C_6F_5$) **[10]**$^-$

	ρ^d	A_s[a]	A_s/Q_d	$\langle A\rangle$[a]
[3e]$^-$	0.51	−73.8	0.56	−73.0
[9]$^-$	0.51	−83.8	0.64	−69.6
[10]$^-$	0.53	−79.5	0.61	−72.0

[a] In units of 10^{-4} cm^{-1}.

shoulders in the low temperature spectra cannot be unambigously assigned, it is apparent that all of the ^{59}Co hyperfine interaction tensor elements are much smaller than in the anions. This is consistent with a mainly ligand centered radical. The formation of substituted cobaltocenium derivatives from **[3e]**$^+$ on standing in solution (i.e. the uptake of a hydrogen or chlorine radical at C-6 of the fulvene) lends chemical evidence for this conclusion and also points to a SOMO localized on the fulvene ligand.

The observed potentials for the first oxidations and reductions also correlate with the idea of reduction taking place mainly at the metal atom, and oxidation at the fulvene ligands. For example, methyl substitution at the C_5H_5 ligand, which pushes electron density onto the metal [28], induces a marked cathodic shift of the first reduction potential. The first oxidation potential is only little affected (compare **3e** with **9**, Table 4). In contrast, oxidation becomes more difficult in **3f**, where the nitro group pulls out electron density from the fulvene ligand.

2.4. Theoretical calculations

Extended Hückel (EH) molecular orbital calculations were carried out on the model complex [(C_5H_5)Co(pentafulvene)] **3h**. Geometrical and computational details are given in Section 3. As a convenient starting point, a geometry was chosen for **3h** which had the fulvene with a planar regular five-membered ring symmetrically η^5-coordinated to the (C_5H_5)Co fragment. An interaction diagram for the construction of the orbitals of **3h** is shown in Fig. 8. For neutral **3h** as well as the radical ions **[3h]**$^-$ and **[3h]**$^+$ the effects were studied when the fulvene ring was independently folded along C1···C4 by an angle φ and translated by a distance d parallel to the plane of the C_5H_5 ring.

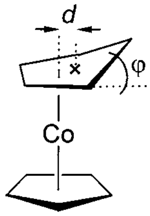

The electronic structure of pentafulvene **1h** has been studied extensively by MO methods. A comparison of several semi-empirical and ab initio calculations has appeared [29]. All calculations give a consistent description of pentafulvene and its 6,6-dialkyl and 6,6-diaryl derivatives as typical polyenes **1**(**A**). The valence orbitals of the (C_5H_5)Co fragment have also been discussed in detail elsewhere [30]. The most important orbital interactions between this fragment and the fulvene ligand are those between the (C_5H_5)Co 2e and $2a_1$ orbital sets, which are hybridized out away from the C_5H_5 ligand, and the π orbitals of fulvene, as shown in Fig. 8.

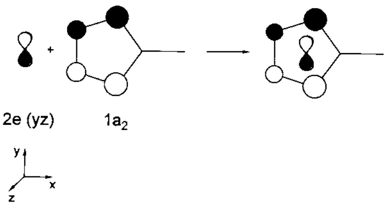

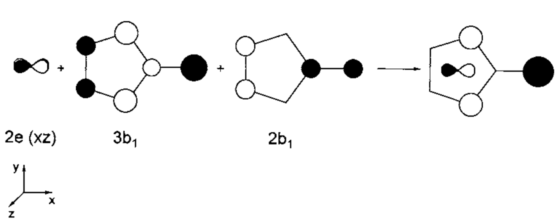

One member of the 2e set on (C_5H_5)Co (d_{yz}) forms a strong bonding combination with a_2 on fulvene. Interaction of these orbitals in the antibonding fashion, shown above, gives the LUMO 13a″ of the complex **3h**. This orbital has a high metal contribution (see below). The bonding combination of (C_5H_5)Co 2e (d_{xz}) with the empty fulvene $3b_1$ orbital is destabilized by an antibonding admixture of $2b_1$ on fulvene (see above). The resulting MO, 20a′, is essentially non-bonding and forms the HOMO of **3h**. This orbital has a large amplitude (essentially p_z) on the *exo* methylene carbon atom C-6 of the fulvene ligand. Both folding and slip of the fulvene ligand decrease the energy of the HOMO, by an increase of the bonding and a decrease of the antibonding interactions. The energy of the LUMO is also lowered by the slip distortion, but is increased by a larger folding. Hence, we expect to find the smallest φ and d in the cation **[3h]**$^+$, where 20a′ is half populated.

Interestingly, within reasonable ranges for the parameters φ (−10–20°) and d (−0.20–0.30 Å) the total one-electron energy of the complex varied little, only by about 0.2 eV for **3h** and **[3h]**$^+$, and by 0.35 eV for **[3h]**$^-$. Optimized values were $\varphi = 8°$, $d = 0.22$ Å for the neutral **3h**, $\varphi = 4°$, $d = 0.12$ Å for **[3h]**$^+$ and $\varphi = 6°$, $d = 0.34$ Å for **[3h]**$^-$ [31]. Mulliken overlap populations for the optimized structures are given in Scheme 1. No bond appears to be present between the cobalt atom and C-1 of the fulvene ligand in **3h** and **[3h]**$^-$, corresponding to an η^4-coordinated ligand. In **[3h]**$^+$, the slightly positive overlap population for these two atoms seems to indicate a weak bonding interaction. However, due to the shallow energy minimum, this difference may not be real [32].

Mulliken atomic charges as calculated for the optimized structures are shown in Scheme 2. Although the actual numbers must be taken carefully, owing to the approximate nature of the method used, the trend is clear. Coordination to the (C_5H_5)Co fragment induces

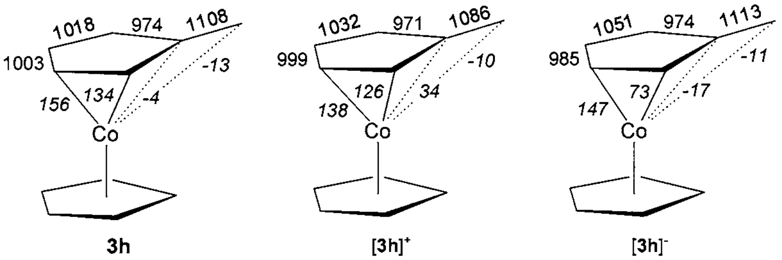

Scheme 1. Mulliken overlap populations [× 10^3] in $[(C_5H_5)Co(pentafulvene)]^n$ ($n = 0, +1, -1$). Values for the cobalt carbon interactions are written in italics.

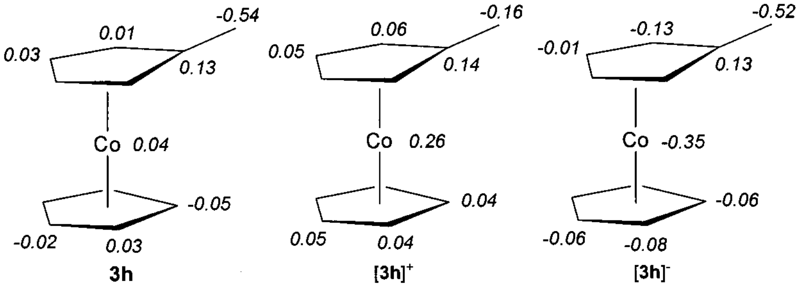

Scheme 2. Calculated charge distribution in $[(C_5H_5)Co(pentafulvene)]^n$ ($n = 0, +1, -1$).

a strong polarization of the fulvene, the negative charge building up mainly on the exocyclic carbon atom C-6. This is in the direction opposite to that observed in free fulvenes with strong electron donors (e. g. an amino group) on C-6, where negative charge accumulates on the five-membered ring, effectively generating a 6π-system [33]. We note here that such ligands coordinate in a η^5 fashion to 12 VE $(CO)_3(d^6\text{-}M)$ fragments to give internal iminium and amidinium salts [34].

One-electron reduction and oxidation of the complex affect the net charges both on the metal and on the fulvene ligand (Scheme 2). Compared with the neutral complex, ca. 0.5 electrons are removed from the fulvene ligand in **[3h]**$^+$, resulting in a greatly reduced negative charge on C-6 in the radical cation. Upon reduction of **3h**, ca. 0.3 electrons are transferred essentially to the carbon and hydrogen atoms of the five-membered ring of the fulvene ligand in **[3h]**$^-$, without changing significantly the net charges on C-1 and C-6.

To get more reliable orbital energies Fenske–Hall approximate SCF-MO calculations were carried out for **3h**, **[3h]**$^+$ and **[3h]**$^-$ in two different molecular geometries, with the fulvene ligand in the planar, η^5-coordinated and the approximately η^4-coordinated geometry, respectively. Compositions of the relevant orbitals are given in Table 7. Regardless of the coordination geometry of the fulvene ligand, a high metal content (about 60%) is calculated for the HOMO of the radical anion **[3h]**$^-$. An estimation of the g tensor for **[3h]**$^-$, using Eqs. (1)–(3) and the eigenvalues and eigenvectors obtained from the Fenske–Hall calculations, gave the odering $\Delta g_x > \Delta g_y > \Delta g_z$ and $\Delta g_z < 0$. This is consistent with the observed spectra although the experimental values of these parameters in **3e** and **9** were not reproduced particularly well. A negative contribution to any Δg_i can only be caused by empty orbitals with high metal content energetically close to the SOMO. The only such orbital in **[3h]**$^-$ is the SOMO + 1 (i.e. the LUMO of the anion), which is only about 0.5 eV above the SOMO. The high d_{xz} content of this orbital accounts for the large negative value of Δg_z.

The HOMO of the radical cation **[3h]**$^+$ has a large amplitude on the exocyclic fulvene carbon atom C-6 and a much smaller metal content. For this orbital, the relative contribution of the atomic orbitals on these atoms are more dependent on the coordination geometry of the fulvene ligand (Table 7).

Clearly, the ESR spectra of **[3e]**$^+$, **[3e]**$^-$ and **[9e]**$^+$, **[9e]**$^-$ are well-accounted for by the theoretical calculations. In particular, the anions are essentially 19 VE complexes with a large cobalt content of the SOMO. The singly occupied molecular orbital of the cations is much more ligand centered (localized to a large extent on fulvene C-6); this is consistent with a much smaller spin–orbit coupling and cobalt hyperfine interaction in the ESR spectra.

3. Experimental

3.1. General procedures

All operations were carried out under an atmosphere of purified nitrogen (BASF R3-11 catalyst) using

Schlenk techniques. Solvents were dried by conventional methods. The complexes $[(C_5H_5)Co(6,6\text{-}R_2C_6H_4)]$ **3e** (R = Ph) [6], **3c** (R = Et) [9], $[(C_5R_5)Co(C_2H_4)_2]$ **8a** (R = H) [35], **8b** (R = Me) [36] and the fulvene ligands 6,6-R,R′-C_6H_4 **1d** (R = Me, R′ = Ph) [15], **1e** (R = R′ = Ph) [15], **1f** (R = Ph, R′ = p-$NO_2C_6H_4$) [37], and **1g** (R = R′ = SMe) [38] were prepared as described in the literature. Petroleum ether refers to the fraction with b.p. 30–60°C. NMR spectra were obtained on Bruker AC 200 or AC 300 instruments (200.1 or 300.1 MHz for ^{1}H, 50.3 MHz for ^{13}C). ^{1}H and ^{13}C chemical shifts are reported versus $SiMe_4$ and were determined by reference to internal $SiMe_4$ or residual solvent peaks. The multiplicities of the ^{13}C resonances [odd (u) or even (g)] were determined using the DEPT or the J-modulated (JMOD) spin echo techniques. ESR spectra were recorded on a Varian E6 spectrometer in the X-band (9.3 GHz). The spectra were calibrated with a LiTCNQ standard, $\langle g \rangle = 2.0025$. Simulation of the anisotropic spectra was carried out with the program SimFonia [39] using second-order perturbation theory. Mass spectra were measured in the electron impact ionization mode at 70 eV on a Finnigan MAT 8230 instrument. Electrochemical experiments were carried out using a EG&G PARC model 173 potentiostat and a model 175 Universal Programmer; a platinum disk working electrode was employed. Redox potentials are referenced to the standard calomel electrode (SCE). Elemental analyses were performed locally by the microanalytical laboratory of the organisch-chemisches Institut der Universität Heidelberg.

*3.2. [(η-Cyclopentadienyl)cobalt(6-methyl-6-phenylpentafulvene)] (**3d**)*

A 800 mg (4.77 mmol) sample of 6-methyl-6-phenylfulvene **1d** was added to a stirred solution of 860 mg (4.77 mmol) of **8a** in 50 ml of petroleum ether at room temperature. A gas evolved and a the solution turned red. After stirring for 15 h, a small amount of a dark precipitate was removed by filtration. The product did not crystallize from petroleum ether, toluene or diethyl ether solutions at −25°C, and could only be obtained as a very air sensitive deep red oil after complete removal of solvent in vacuo.

^{1}H-NMR (200 MHz, in C_6D_6): $\delta = 1.86$ (s, 3H, Me), 3.91 (br.s, 1H, CH), 4.420 (s, 5H, C_5H_5), 4.425 (s, 1H, CH), 4.96 (br.s, 1H, CH), 5.04 (br.s, 1H, CH), 7.01 (m, 1H, Ph), 7.27 (m, 2H, Ph), 7.46 (m, 2H, Ph). $^{13}C\{^1H\}$-NMR (in C_6D_6): $\delta = 19.5$ (Me), 55.8 (C-2 or C-5), 58.0 (C-5 or C-2), 77.0 (C-3 or C-4), 77.6 (C-4 or C-3), 78.9 (C_5H_5), 98.6 (C-1), 123.7 (g, Ph), 126.8 (g, Ph), 128.5 (g, Ph), 145.5 (u, C-6). Reliable microanalyses could not be obtained due to the high air sensitivity of the liquid product.

*3.2 [(η-Cyclopentadienyl)cobalt(6-phenyl-6-p-nitrophenylpentafulvene)] (**3f**)*

A mixture of 970 mg (4.82 mmol) of **8a** and 1.09 g (4.82 mmol) of 6-p-nitrophenyl-6-phenylfulvene **1f** in 60 ml of toluene was stirred at room temperature. The mixture quickly turned blue and evolution of a gas was

Table 7
Composition (%) of the frontier molecular orbitals for the model complexes $[(C_5H_5)Co(C_5H_4CH_2)]^n$ **3h** as derived from Fenske–Hall MO calculations

n	Orbital	Energy (eV)	Co 3d	Co 4s	Co 4p	C-1	C-2	C-3	C-6
Fulvene ligand planar									
0	HOMO	−7.70	20.5[a]	0.5	2.0	2.3	2.3	0	60.0
0	LUMO	−4.27	51.7[b]	0	0.6	0	8.9	2.2	0
0	LUMO+1	−2.99	34.8[a]	0.02	3.4	0	5.7	7.4	14.3
−1	SOMO	2.54	60.5[b]	0	0.6	0.3	7.6	1.7	0
−1	LUMO	3.56	45.8[a]	0	2.9	3.8	5.1	6.9	8.5
+1	SOMO	−14.77	17.7[a]	0.6	3.6	0.2	3.7	0.4	57.6
Fulvene ligand bent									
0	HOMO	−9.03	30.0[a]	1.1	5.4	1.8	5.9	0.9	37.7
0	LUMO	−3.50	52.3[b]	0	1.06	0.5	9.3	2.8	0.01
0	LUMO+1	−2.64	33.6[a]	0	2.7	4.8	6.0	8.2	15.2
−1	SOMO	3.35	61.2[b]	0	1.0	0.5	8.1	2.1	0.01
−1	LUMO	3.89	44.5[a]	0	2.0	5.6	4.5	7.3	10.8
+1	SOMO	−15.50	26.7[a]	1.1	6.8	1.1	6.4	1.1	34.5

[a] Mainly $3d_{xz}$.

[b] Mainly $3d_{yz}$.

observed. After 15 h, a large amount of a dark intractable precipitate was removed by filtration. Solvent was removed from the blue filtrate in vacuo, and the residue redissolved in CH_2Cl_2. Petroleum ether was added, and the solution was cooled to -25°C. A first crop of the product **3f** precipitated as a blue powder after several days. Further product fractions were obtained from the mother liquor by repeating the above procedure. Total yield 380 mg (20%).

^{1}H-NMR (200 MHz, in C_6D_6): $\delta = 4.27$ (m, 1H, CH), 4.30 (s, 5H, C_5H_5), 4.46 (m, 1H, CH), 4.64 (m, 1H, CH), 4.72 (m, 1H, CH), 6.98–7.17 (m, 5H, Ph), 7.13 and 8.09 (m, AA′BB′ pattern, 2 × 2H, C_6H_4). $^{13}C\{^1H\}$-NMR (in C_6D_6): $\delta = 78.8$ (g, CH), 80.3 (g, C_5H_5), 81.4 (g, CH), 102.7 (u, C-1), 124.1 (g, CH), 125.9 (g, CH), 126.7 (g, CH), 129.0 (g, CH), 131.0 (g, CH), 141.0 (u, C), 144.1 (u, C), 150.8 (u, C). MS: $m/z = 399$ (53%, M^+), 370 (7), 351(8), 293 (11), 275 (100, $[M - C_5H_5Co]^+$), 229 (58, $[L - NO_2]^+$), 228 (94), 226 (58), 215 (13), 202 (30), 189 (12, $[Co(C_5H_5)_2]^+$), 153 (8, $[L - C_6H_4NO_2]^+$), 152 (10), 150 (6), 124 (4, $[Co(C_5H_5)]^+$), 120 (7), 114 (7), 105 (9) (L = 6-*p*-nitrophenyl-6-phenylfulvene). Anal. Calc. for $C_{23}H_{18}CoNO_2$ (399.33): C, 69.18; H, 4.54; N, 3.51; Found: C, 68.18; H, 4.76; N, 3.37.

3.4. [(η-Cyclopentadienyl)cobalt(6,6-bis(methylmercapto)pentafulvene)] (3g)

A 570 mg (3.3 mmol) sample of bis(methylmercapto)fulvene **1g** was added to a stirred solution of 600 mg (3.3 mmol) of **8a** in 50 ml of petroleum ether at room temperature. A gas evolved and a red solid precipitated. After standing for 36 h the mother liquor was decanted from the precipitate, which was then recrystallized from toluene. The product **3g** (580 mg, 60%) crystallized as red platelets at -6°C, m.p. 88°C.

^{1}H-NMR (300 MHz, C_6D_6): $\delta = 2.25$ (s, 6H, CH_3), 4.30 (s, 5H, C_5H_5), 4.71 (m, 4H, CH). $^{13}C\{^1H\}$-NMR (in C_6D_6): $\delta = 16.8$ (g, CH_3), 59.0 (g, CH), 77.2 (g, CH), 80.0 (g, C_5H_5), 139.7 (u, C-6). MS: $m/z = 294$ (25%, M^+), 279 (100, $[M - CH_3]^+$), 246 (15), 232 (24, $[M - SMe_2]^+$), 188 (9), 169 (14), 124 (11, $[Co(C_5H_5)]^+$), 116 (14), 59 (9, Co^+). Anal. Calc. for $C_{13}H_{15}CoS_2$ (294.32): C, 53.05; H, 5.14; Found: C, 52.79; H, 5.26.

3.5. [(η-Pentamethylcyclopentadienyl)cobalt(6,6-diphenylpentafulvene)] (9)

A petroleum ether solution (60 ml) of 740 mg (2.96 mmol) of **8b** and 680 mg (2.96 mmol) of 6,6-diphenylfulvene **1e** was stirred at room temperature for 18 h. After filtration, the volume of the deep red mixture was reduced in vacuo to about half. On cooling to -25°C, the product **9** (820 mg, 65%) crystallized as deep red cubes, m.p. 108°C.

^{1}H-NMR (200 MHz, in C_6D_6): $\delta = 1.51$ (s, 15H, Me), 3.96 (m, 2H, H-2/H-5), 4.36 (m, 2H, H-3/H-4), 7.00–7.57 (m, 10H, Ph). $^{13}C\{^1H\}$-NMR (in C_6D_6): $\delta = 10.2$ (g, C_5Me_5), 63.0 (g, C-3/C-4 or C-2/C-5), 78.0 (g, C-2/C-5 or C-3/C-4), 90.2 (u, C_5Me_5), 99.7 (u, C-1), 123.7 (g, Ph), 127.2 (g, Ph), 130.1 (g, Ph), 146.0 (u, C-6). MS: $m/z = 424$ (100%, M^+), 409 (24, $[M - CH_3]^+$, 229 (5, $[Ph_2C_6H_3]^+$), 212 (20), 57 (5). Anal. Calc. for $C_{28}H_{29}Co$ (424.47): C, 79.23; H, 6.89; Found: C, 79.09; H, 7.03.

3.6. [(η-Cyclopentadienyl){η-(pent-3-yl)cyclopentadienyl} cobalt ([3c + H]$^+$)

A 260 mg (1.01 mmol) sample of **3c** in 10 ml of diethyl ether was treated with 0.5 ml HBF_4 (80% in diethyl ether). The mixture was stirred at ambient temperature for 30 min. The colourless ether phase was then decanted from a brown oil, which was repeatedly washed with ether and then dissolved in acetone. A solution of $NaBPh_4$ (340 mg, 1 mmol) in 10 ml of acetone was added. On cooling of the mixture to -25°C, the product $[\mathbf{3c} + H]^+$ (350 mg, 60%) crystallized as dark needles.

^{1}H-NMR (200 MHz, in CD_2Cl_2): $\delta = 0.89$ (t, 6H, Me), 1.62 (m, 4H, CH_2), 2.38 (m, 1H, H(C-α)), 5.53 (m, 2H, H-2/H-5 or H-3/H-4), 5.65 (s, 5H, C_5H_5), 5.68 (m, 2H, H-3/H-4 or H-2/H-5). $^{13}C\{^1H\}$-NMR (in CD_2Cl_2): $\delta = 10.0$ (g, CH_3), 25.7 (u, CH_2), 39.1 (g, C-α), 82.6 (g, C-2/C-5 or C-3/C-4), 82.9 (g, C-3/C-4 or C-2/C-5), 84.8 (g, C_5H_5), 85.1 (u, C_{ipso}). FD-MS: $m/z = 259$ (100%, M^+).

3.7. X-ray crystal structure determinations of [(C_5H_5)Co{6,6-bis(mercaptomethyl)fulvene}] 3g, [(C_5Me_5)Co(6,6-diphenylfulvene)] 9 and [(C_5H_5)Co{$C_5H_5C(H)Ph_2$}][PF_6] [3e + H]$^+$[PF_6]$^-$

Single crystals of **3g** and **9** were obtained from hexane solutions at -20°C. The salt $[\mathbf{3e} + H]^+[PF_6]^-$ was prepared from **3e** and HPF_6; crystallization from a methylene chloride solution at 6°C gave single crystals. The crystals were mounted in Lindemann capillary tubes and transferred to a STOE-Siemens four circle diffractometer. Intensity data were collected at ambient temperature and corrected for Lorentz, polarization and absorption effects (Table 8). The structures were solved by the Patterson or direct methods and refined on F^2 with full-matrix least-squares using all measured unique reflections. All non-hydrogen atoms in **3g**, **9** and $[\mathbf{3e} + H]^+[PF_6]^-$ were given anisotropic displacement parameters (ADPs). For complex **3g**, all hydrogen atoms were located from difference Fourier syntheses and refined with isotropic ADPs. For the complexes **9** and $[\mathbf{3e} + H]^+[PF_6]^-$ the hydrogen atoms were inserted in calculated positions [40].

Table 8
Details of the crystal structure determinations of [(η-C_5R_5)Co(6,6-$R'_2C_6H_4$)] **3g** (R = H, R′ = SMe), **9** (R = Me, R′ = Ph) and [(η-C_5H_5)Co{$C_5H_4C(H)Ph_2$}]$^+$[PF_6]$^-$ [**3e**+H]$^+$[PF_6]$^-$

	3g	**9**	[**3e**+H]$^+$[PF_6]$^-$
Formula	$C_{13}H_{15}CoS_2$	$C_{28}H_{29}Co$	$C_{23}H_{20}CoF_6P$
Crystal system	Orthorhombic	Monoclinic	Monoclinic
Space group	*Pbca*	$P2_1/n$	$P2_1/n$
a (Å)	7.502(4)	8.960(6)	9.062(7)
b (Å)	17.143(9)	25.082(12)	22.670(16)
c (Å)	20.264(10)	10.590(8)	10.757(8)
β (°)	90	107.20(3)	103.71(6)
V (Å^3)	2606(2)	2274(3)	2147(3)
Z	8	4	4
M_r	294.32	424.47	500.29
d_c (g cm^{-1})	1.500	1.240	1.548
F_{000}	1216	896	1016
μ(Mo–K_α) (cm^{-1})	1.61	0.77	0.93
X-radiation, λ (Å)	Mo–K_α, graphite monochromated, 0.71069		
Data collect. temperature	Ambient	Ambient	Ambient
2ϑ range [°]	3–50	3–51	3–47
hkl-range			
h	0–8	−10–10	−10–9
k	0–20	0–29	0–25
l	0–24	0–12	0–12
Reflections measured			
Unique	2291	4142	3152
Observed [$I \leq 2\sigma(I)$]	1514	2895	1676
Absorption correction	Empirical	Empirical	Empirical
Parameters refined	184	271	288
R-values			
R (obs. reflections only)	0.039	0.045	0.059
wR_2 (all reflections)	0.092	0.117	0.211
($w = 1/[\sigma^2(F)+(A \cdot P)^2+B \cdot P]$,			
A, *B*	0.0307, 0.76	0.0575, 0.54	0.0518, 2.81
P	max(F_o^2, 0)+2F_c^2)/3)		
GoF	1.016	1.036	1.402
Largest/smallest peak in difference-Fourier (e Å^{-3})	0.26/−0.45	0.33/−0.25	0.45/−0.31

The calculations were performed using the programs SHELXS-86 and SHELXL-93 [41]. Graphical representations were drawn with the SCHAKAL-92 program [42].

3.8. Molecular orbital calculations

Extended Hückel calculations [43] were carried out with CACAO [44] using the wavefunctions supplied with the package. The basis set for the metal atom consisted of *n*s, *n*p, and (*n* − 1) d orbitals. The s and p orbitals were described by single Slater-type wave functions, and the d orbitals were taken as contracted linear combinations of two Slater-type wave functions. The weighted Wolfsberg–Helmholtz formula [45] was employed. The iterative self-consistent field Fenske–Hall procedure [46] is an approximation [47] of the Hartree–Fock–Rothaan method and employs the atomic basis functions and the molecular geometry as the only adjustable parameters. The STO basis functions used in the FH calculations have been developed by the Fenske group using the numerical Xα atomic orbital program of Herman and Skilman [48] in conjunction with the Xα-to-Slater basis program of Bursten and Fenske [49]. Exponents of 4s and 4p atomic orbitals for cobalt were set to 2.0. These functions are less diffuse than the atomic functions but lead to a better description of the bonding in organometallic complexes [50]. A value of 1.20 was used for the hydrogen exponent. Idealized models were used for the complexes studied. The unpaired electron in the 'open-shell' systems was treated as two half-electrons of opposite spin [51]. The geometry of **3h** was set up with C_s molecular symmetry. The following distances (Å) were used: Co–C(C_5H_5) 2.06, Co–fulvene(normal) 1.68, C–C 1.40, C–H 1.08.

Acknowledgements

This work was supported by the Deutsche Forschungsgemeinschaft under the auspices of the Sonderforschungsbereich 247 of the Universität Heidelberg and by the Fonds der Chemischen Industrie. A Heisenberg fellowship to H.W. is gratefully acknowledged.

References

[1] D. Lloyd, Non-Benzenoid Conjugated Carbocyclic Compounds, Elsevier, Amsterdam, 1984.

[2] (a) P.A. Straub, D. Meuche, E. Heilbronner, Helv. Chim. Acta 49 (1966) 517. (b) E.D. Bergmann, Chem. Rev. 68 (1968) 41.

[3] R.C. Kerber, D.J. Ehntholt, Synthesis (1970) 449.

[4] E. Weiss, W. Hübel, Chem. Ber. 95 (1962) 1186.

[5] F. Edelmann, B. Lubke, U. Behrens, Chem. Ber. 115 (1982) 1325.

[6] H. Wadepohl, Habilitationsschrift, Universität Heidelberg, 1989.

[7] D. Rau, U. Behrens, J. Organomet. Chem. 387 (1990) 219.

[8] H. Wadepohl, H. Pritzkow, Acta Crystallogr. Sect. C 47 (1991) 2061.

[9] H. Wadepohl, C.-W.v.d. Lieth, F.-J. Paffen, H. Pritzkow, Chem. Ber. 128 (1995) 317.

[10] (a) H. Wadepohl, H. Pritzkow, Angew. Chem. 99 (1987) 132. (b) H. Wadepohl, W. Galm, H. Pritzkow, A. Wolf, J. Chem. Soc. Chem. Commun. (1993) 1459. (c) H. Wadepohl, W. Galm, H. Pritzkow, A. Wolf, Chem. Eur. J. 2 (1996) 1453.

[11] J.E. Sheats, W. Miller, T. Kirsch, J. Organomet. Chem. 91 (1975) 97.

[12] H.F. Klein, E. Auer, T. Jung, C. Röhr, Organometallics 14 (1995) 2731.

[13] D.W. Hoard, P.R. Sharp, Inorg. Chem. 32 (1993) 612.

[14] D.S. Glueck, R.G. Bergman, Organometallics 9 (1990) 2862.

[15] K.P. Zeller, in: H. Kropf (ed.), Methoden der Organischen Chemie (Houben-Weyl), Vol. 5/2c, Thieme, Stuttgart 1985, and references cited therein.

[16] J.R. Bleeke, R.R. Burch, C.L. Coulman, B.C. Schardt, Inorg. Chem. 20 (1981) 1316.

[17] O. Koch, F. Edelmann, U. Behrens, Chem. Ber. 115 (1982) 1305.

[18] (a) H.v. Willigen, W.E. Geiger Jr., M.D. Rausch, Inorg. Chem. 16 (1977) 581. (b) T.A. Albright, W.E. Geiger Jr., J. Moraczewski, B. Tulyathan, J. Am. Chem. Soc. 103 (1981) 4787. (c) W.E. Geiger, T. Gennett, M. Grzeszczuk, G.A. Lane, J. Moraczewski, A. Salzer, D.E. Smith, J. Am. Chem. Soc. 108 (1986) 7454. (d) L. Vasquez, H. Pritzkow, U. Zenneck, Angew. Chem. 100 (1988) 705. (e) B.L. Ramakrishna, A.K. Salzer, U. Ruppli, J.H. Ammeter, U. Kölle, Inorg. Chem. 25 (1986) 1364.

[19] P.H. Rieger, in: W.C. Trogler (ed.), Organometallic Radical Processes, Elsevier, Amsterdam, 1990, chapter 8.

[20] J.R. Morton, K.F. Preston, J. Magn. Reson. 30 (1978) 577.

[21] P. Coppens, T. Koritsanszky, P. Becker, Chem. Scr. 26 (1986) 463.

[22] B.M. Peake, P.H. Rieger, B.H. Robinson, J. Simpson, J. Am. Chem. Soc. 102 (1980) 156.

[23] J.H. Bieri, A.S. Dreiding, T.C.C. Gartenmann, E.R.F. Gesing, R.W. Kunz, R. Prewo, J. Organomet. Chem. 306 (1986) 241.

[24] D.R. Tyler, Acc. Chem. Res. 24 (1991) 325.

[25] W.E. Geiger, Acc. Chem. Res. 28 (1995) 351.

[26] W.E. Geiger, P.H. Rieger, C. Corbato, J. Edwin, E. Fonseca, G.A. Lane, J.M. Mevs, J. Am. Chem. Soc. 115 (1993) 2314.

[27] W.E. Geiger, T. Gennett, G.A. Lane, A. Salzer, A.L. Rheingold, Organometallics 5 (1986) 1352.

[28] D.C. Calabro, J.L. Hubbard, C.H. Blevins II, A.C. Campbell, D.L. Lichtenberger, J. Am. Chem. Soc. 103 (1981) 6839.

[29] K.N. Houk, J.K. George, R.E. Duke, Tetrahedron 30 (1974) 523.

[30] M. Elian, M.M.L. Chen, D.M.P. Mingos, R. Hoffmann, Inorg. Chem. 15 (1976) 1148.

[31] For comparison, EH calculations were also carried out for the complex $[(C_5H_5)Co(C_5H_6)]$ with the geometric parameters φ and d defined as for **3h**. Not surprisingly, this structure optimized to a deeper minimum at larger φ and d, 25° and 0.25 Å, respectively, than those obtained for **3h**, corresponding to an η^4-coordinated cyclopentadiene ligand.

[32] In a structure of **3h** where the coordination geometry of the fulvene ligand was forced to η^5 (i.e. symmetrical bonding of the C_5 ring of a planar fulvene to the cobalt atom), the overlap population Co–C(1) came out only about half that of Co–C(2) through to C(5). This quantity was only slightly dependent on the molecular charge (increased by 0.005 in the cation, decreased by 0.008 in the anion).

[33] K. Hafner, K.H. Häfner, M. Kreuder, G. Ploss, G. Schulz, E. Sturm, K.H. Völpel, Angew. Chem. 75 (1963) 35.

[34] P. Bickert, B. Hildebrandt, K. Hafner, Organometallics 3 (1984) 653 and references cited therein.

[35] K. Jonas, E. Deffense, D. Habermann, Angew. Chem. 95 (1983) 729; Angew. Chem. Suppl. (1983) 1005.

[36] S.A. Frith, J.L. Spencer, Inorg. Synth. 23 (1985) 15.

[37] G. Kresze, S. Rau, G. Satelus, H. Goetz, Liebigs Ann. Chem. 648 (1961) 51.

[38] R. Gompper, E. Kutter, Chem. Ber. 98 (1965) 2825.

[39] WINEPR SimFonia, version 1.25, Bruker Analytische Meßtechnik, Karlsruhe, 1996.

[40] (a) SHELXS-86, G.M. Sheldrick, Acta Cryst. A46 (1990) 467. (b) SHELXL-93, G.M. Sheldrick, Universität Göttingen 1993.

[41] Crystallographic data (excluding structure factors) for the structures reported in this paper have been deposited with the Cambridge Crystallographic Data Centre as supplementary publication Nos. CCDC 113629 (**3g**), 113630 (**9**) and 113631 ($[\mathbf{3e}+H]^+$). Copies of the data can be obtained free of charge on application to The Director, CCDC, 12 Union Road, Cambridge CB2 1EZ, UK (Fax: +44-1223-336-033; e-mail: teched@chemcrys.cam.ac.uk).

[42] SCHAKAL-92, E. Keller, Universität Freiburg, 1992.

[43] (a) R. Hoffmann, J. Chem. Phys. 39 (1963) 1397. (b) R. Hoffmann, W.N. Lipscomb, J. Chem. Phys. 36 (1962) 2179, 3489.

[44] C. Mealli, D.M. Proserpio, J. Chem. Edu. 67 (1990) 39.

[45] J.H. Ammeter, H.-B. Bürgi, J.C. Thibeault, R. Hoffmann, J. Am. Chem. Soc. 100 (1978) 3686.

[46] (a) M.B. Hall, R.F. Fenske, Inorg. Chem. 11 (1972) 768. (b) R.F. Fenske, Pure Appl. Chem. 60 (1988) 1153.

[47] B.E. Bursten, Pure Appl. Chem. 63 (1991) 839.

[48] F. Herman, S. Skillman, Atomic Structure Calculations, Prentice-Hall, Englewood Cliffs, NJ, 1963.

[49] (a) B.E. Bursten, R.F. Fenske, J. Chem. Phys. 67 (1977) 3138. (b) B.E. Bursten, R.J. Jensen, R.F. Fenske, J. Chem. Phys. 68 (1978) 3320.

[50] R.F. Fenske, D.D. Radtke, Inorg. Chem. 7 (1968) 479.

[51] T.F. Block, R.F. Fenske, C.P. Casey, J. Am. Chem. Soc. 98 (1976) 441.